Proceedings of the 17th Japan-Taiwan International Workshop on Hydrological and Geochemical Research for Earthquake Prediction

4 September, 2018
GSJ, AIST, Tsukuba, Japan

Norio Matsumoto and Chjeng-Lun Shieh eds.

DPRC Disaster Prevention Research Center
National Cheng Kung University
No.1,Ta-Hsueh Rd. Tainan 701, Taiwan

IEVG
Research Institute of Earthquake and Volcano Geology
GEOLOGICAL SURVEY OF JAPAN
NATIONAL INSTITUTE OF
ADVANCED INDUSTRIAL SCIENCE AND TECHNOLOGY (AIST)
1-1 Higashi 1-Chome, Tsukuba, Ibaraki, 305-8567 Japan
2018

The 17th Japan-Taiwan International Workshop on Hydrological and Geochemical Research for Earthquake Prediction

4 September, 2018

Meeting room No.2, Geological Survey of Japan (GSJ), AIST, Tsukuba, Japan

No	From	To	Name	Presentation
Morning sesson				
	10:00	10:10	Yusaku Yano (Director General of GSJ, AIST)	Greeting
1	10:10	10:30	Mamoru Nakamura (UR)	Seasonal to multi-annual tidal response change of very low-frequency earthquakes induced by atmospheric and oceanic variations
2	10:30	10:50	Min-Chien Tsai (CWB)	Triggering of multifault ruptures after 2018 Mw 6.4 offshore Hualien earthquake: Insight from geodetic measurements and SAR interferometry.
3	10:50	11:10	Jyr-Ching Hu (NTU)	Reassess coseismic and postseismic slip on triggered shallow slip of 2016 Mw 6.4 Meinong earthquake by high-rate GPS, campaign GPS, InSAR and strong motion observation,
4	11:10	11:30	Masayuki Murase (NU)	Vertical deformation of the 2017 M5.6 earthquake detected by precise leveling in the Ontake earthquake swarm area, central Japan
	11:30	11:40	Coffee break	
5	11:40	12:00	Yuzo Ishikawa (AIST)	Eruptions and earthquakes in Hawaii Island
6	12:00	12:20	Xinglin Lei (AIST)	Case studies of long- and short-term injection-induced earthquakes
	12:20	12:40	Group Photo at the 1st floor of the building	
	12:40	13:40	Lunch (Lunch Meeting for presenters at Meeting Room No.1 at 8th floor)	
Afternoon session #1				
7	13:40	14:00	Hitomi Nakamura (AIST)	Geochemical variability of deep seated fluid along median tectonic line
8	14:00	14:20	Shih-Jung Wang (NCU)	Using Post-seismic Groundwater Recovery Data to Estimate the Hydraulic Properties of Aquitards
9	14:20	14:40	Norio Matsumoto (AIST)	Comparison of Permeability of Fault Zone Between In-situ Hydraulic Tests and Laboratory-Derived Data at the Median Tectonic Line, Central Japan
10	14:40	15:10	Masao Nakatani (ERI, UT)	Statistical evaluation of precursory phenomena – A review
11	15:10	15:30	Yasuyuki Kano (ERI, UT)	Connection between historical earthquake and groundwater anomaly
	15:30	15:50	Coffee break and Poster session	
Afternoon session #2				
12	15:50	16:10	Taku Nakamura (GU)	Observation of Water in Wariishi Hot Spring
13	16:10	16:30	Yang Li (NU)	The earthquake related water level increase at Oi well in Kanagawa prefecture
14	16:30	16:50	Ching-Chou Fu (IES, AS)	Changes in groundwater chemistry at the Taiwan Chelungpu Fault Borehole before the 2013 M6.2 Nantou earthquake
15	16:50	17:10	Wen-Chi Lai (DPRC, NCU)	The preliminary study of the coseismic groundwater level changes in ML 6.2 Hulien earthquake, Feb. 6th 2018
16	17:10	17:30	Naoji Koizumi (USP)	Postseismic changes in stream water related to the 2016 Kumamoto earthquake
	17:30	17:50		Discussion
	18:00			Banquet (Restaurant, 2nd Floor of Welfare Building in Tsukuba Central 1)

UR: University of the Ryukyus
IES, AS: Institute of Earth Sciences, Academia Sinica, Taiwan
CWB: Central Weather Bureau, Taiwan,
NTU: National Taiwan University, Taiwan
NCU: National Central University, Taiwan
DPRC，NCKU: Disaster Prevention Research Center, National Cheng Kung University, Taiwan
USP: The University of Shiga Prefecture
NU: Nihon University
GU: Gifu University
ERI, UT: Earthquake Research Institute, University of Tokyo
AIST: National Institute of Advanced Industrial Science and Technology

Contact: Norio Matsumoto： n.matsumoto@aist.go.jp 029-861-2380, 3656 (222-42380, 221-33656)

Seasonal to multi-annual tidal response change of very low-frequency earthquakes induced by atmospheric and oceanic variations

Mamoru Nakamura*[1]

1. Faculty of Science, University of the Ryukyus, Nishihara-cho, Okinawa, Japan

The activity of very low-frequency earthquakes (VLFEs) in the Ryukyu trench, southwestern Japan, is affected by tidal stress. The tidal response of the VLFE is higher in the Amami Islands and Okinawa Islands of the central Ryukyu trench [*Nakamura and Kakazu, 2017*]. The activity reaches its peak during low tide, when the Coulomb failure stress (ΔCFS) in the subducted plate interface reaches its maximum. The amplitude of the tidal response (ATR) exhibits seasonal variation. The monthly average ATR is small in summer and large in winter. Moreover, the annually averaged ATR changes over several years. The relationship between stress change and the ATR was investigated to clarify the cause of seasonal and multi-annual variation.

The daily ΔCFS was calculated in the plate interface by the loading of atmospheric pressure (AP), rainfall loading (RL), and ocean bottom pressure (OBP), to compare it with the ATR. The daily global grid model was employed for the AP and OBP loading. For the OBP data, ECCO version 4 release 3 [*Forget et al., 2016; Fukumori et al., 2017*] was employed, which is based on the four-dimensional assimilation model. Daily precipitation data by JMA was used for the calculation of RL. The observed precipitation at each observation station was interpolated and converted to the grid data, then the storage and outflow of the rainfall was estimated using the three-storage tank model. The parameters used were those of the tank model of the soil rainfall index developed by JMA [*Osanai et al., 2010*]. The stress in the plate interface was modelled using software with modified SPOTL [*Agnew, 2013*], to be enabled to calculate the stress at any depth by the surface loading.

The result showed that the RMS amplitude of the ΔCFS by AP was on the order of 50 Pa near the island; it decreased abruptly as distance from the island increased. The distribution of the RL was also similar to that of the AP, although the amplitude of the RL was approximately half that of the AP. The RMS amplitude of the delta-CFS by OBP was 10 Pa near the trench axis; it increased to 60 Pa at a depth of 60 km in the subducted plate interface. The amplitude of the ΔCFS by AP+RL+OBP is 60 Pa near the island.

Following this, the seasonal and multi-annual variation of the ATR was computed. Excess events (N_{ex}) were employed for the evaluation of the ATR [*Cochran et al., 2004*]. The result shows that the ATR was at its maximum from October to February, and at its minimum from April to August (Fig. 1b). The annual N_{ex} was 0.25–0.30 during 2003–2006, and 0.33 during 2007–2011 (Fig. 1d). The N_{ex} decreased to 0.23–0.30 after 2011.

The ΔCFS was then converted to the slip velocity change in the plate interface and compared with the ATR. The equation of Tanaka et al. (*2015*) was employed to convert the ΔCFS to slip velocity change. The daily ΔCFS was interpolated to hourly ΔCFS, and converted to slip velocity by adding the ΔCFS by ocean tide and Body tide. The monthly and annual ΔCFSs were calculated using the hourly ΔCFS. Finally, the slip rate and the occurrence of the slow slip events (SSEs) in the Ryukyu Trench were compared.

The results showed that the monthly slip rate by tide+AP+WP+OBP had a moderate correlation (0.4–0.5) to the ATR (Fig. 1a). However, the annual slip rate had a strong correlation (0.7) to ATR (Fig. 1c). Moreover, the fluctuation of the ATR by monthly and annual slip rate change was 5–10 times higher than that by daily slip rate change. This suggests that the sensitivity of slip rate is frequency dependent; the sensitivity by stress perturbation for several months to years is higher than that for half a day to a full day.

The occurrence of SSEs in the Okinawa Islands and Yaeyama Islands were not correlated with the degree of ΔCFS in the source faults of the SSEs. This suggests that stress change by nontidal components affects the occurrence of VLFEs, whereas it does not promote the occurrence of SSEs.

References

Agnew, D. C. (2013). SPOTL: *Some programs for ocean-tide loading*. San Diego, CA: UC San Diego: Scripps Institution of Oceanography. Retrieved from https://igppweb.ucsd.edu/~agnew/Spotl/spotlman.pdf

Cochran, E. S., Vidale, J. E., & Tanaka, S. (2004). Earth tides can trigger shallow thrust fault earthquakes. *Science*, *306*(5699), 1164–1166. https://doi.org/10.1126/science.1103961

Forget, G., Campin, J.-M., Heimbach, P., Hill, C. N., Ponte, R. M., & Wunsch, C. (2016). *ECCO version 4: Second release*. Retrieved from http://hdl.handle.net/1721.1/102062

Fukumori, I., Wang, O., Fenty, I., Forget, G., Heimbach, P., & Ponte, R. M. (2017) *ECCO Version 4 Release 3*. Retrieved from http://hdl.handle.net/1721.1/110380

Nakamura, M., & Kakazu, K. (2017). Tidal sensitivity of shallow very low frequency earthquakes in the Ryukyu Trench. *Journal Geophysical Research: Solid Earth*, *122*(2), 1221–1238. https://doi.org/10.1002/2016JB013348.

Osanai, N., Shimizu, T., Kuramoto, K., Kojima, S., & Noro, T. (2010). Japanese early-warning for debris flows and slope failures using rainfall indices with Radial Basis Function Network. *Landslides*, *7*(3), 325–338. https://doi.org/10.1007/s10346-010-0229-5.

Tanaka, Y., Yabe, S., & Ide, S. (2015). An estimate of tidal and non-tidal modulations of plate subduction speed in the transition zone in the Tokai district. *Earth, Planets and Space*, *67*, 141. https://doi.org/10.1186/s40623-015-0311-2

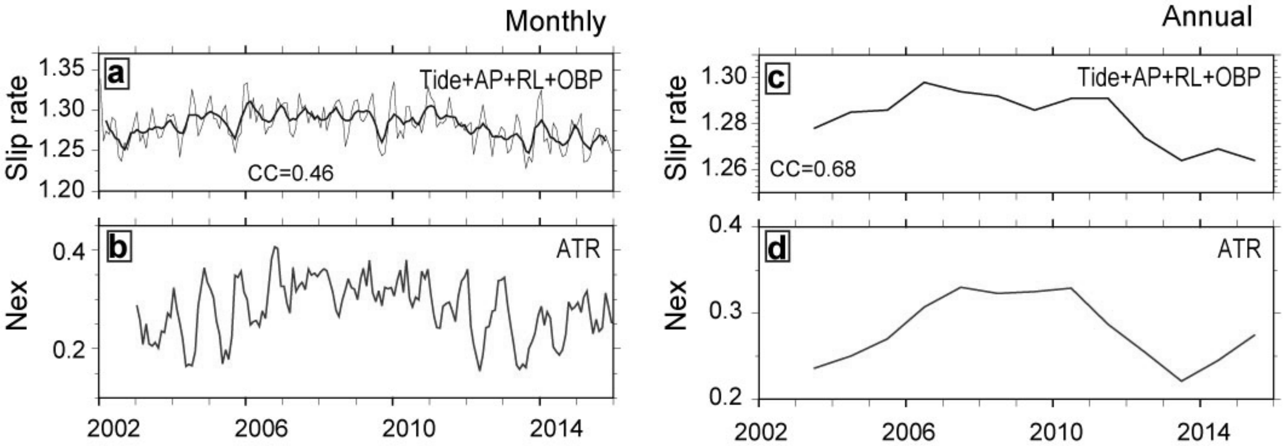

Fig.1. Monthly and long-term variation of slip rates converted from Coulomb failure stress (ΔCFS) and excess events (N_{ex}) south of Okinawa Island. (**a**) Monthly slip rate by tide, atmospheric pressure (AP), rainfall loading (RL), and ocean bottom pressure. Thin and thick lines denote the monthly and four-month moving average monthly slip rate, respectively. CC indicates cross-correlation between the slip rate and monthly N_{ex}. (**b**) Monthly N_{ex}. (**c**) Annual slip rate by tide, AP, RL, and OBP. CC indicates cross-correlation between the slip rate and annual N_{ex}. (**d**) Annual N_{ex}.

Triggering of multifault ruptures after 2018 Mw 6.4 offshore Hualien earthquake: Insight from geodetic measurements and SAR interferometry

Min-Chien Tsai*[1], Ying-Hui Yang[2], and Jyr-Ching Hu[3]

1. Seismological Center, Central Weather Bureau, Taipei, Taiwan, R.O.C. 2. School of Civil Engineering and Architecture, Southwest Petroleum University, Chengdu, China

3. Department of Geosciences, National Taiwan University, Taipei, Taiwan, R.O.C

Two earthquakes of Mw 6.0 and Mw 6.4 occurred at the complex junction of northern extension of collisional boundary and Ryukyu subduction zone on February 4 and 6, separately. Second event was located at about 16.5 km north-east of the Hualien City, the biggest city in Eastern Taiwan, resulting in severe building damage and 17 deaths. The major damage zine was found near the Milun fault. According to the field investigation, surface rupture was found along the Milun fault, an active fault had been rupture by ML 7.1 earthquake in 1951 (Hsu, 1962; Hsu, 1971; Bonilla, 1977, 1979) with a 2 m of left slip and 1.2 m uplift on the southeast of the fault. According to focal mechanism the NE-striking and west-dipping reverse fault dipping with left-lateral slip component could be the seismogenic fault, an alternative fault plane could be a NW-striking and south-dipping reverse fault with right-lateral slip component. However, only minor coseismic deformation was observed around the epicentral and near-field area. Significant coseismic deformation is observed along the NE-striking and east-dipping Milun fault and Footwall of the NE-striking and east-dipping Lingding fault which is the north segment of the Longitudinal Valley fault. Thus the coseismic deformation pattern could be resulted from the mutlifault rupture during the Hualien event. The maximum coseismic deformation reaches to 46 cm in the horizontal component and 9 cm in vertical component. The significant left-lateral strike-slip coseismic deformation dominates along the Milun fault. In addition, the coseismic deformation changes in the southernmost of the Milun fault which implies that the Milun fault and the north segment of the Lingding fault should belong to the different fault systems. It is worthy to note that the larger coseismic uplift is observed along the foot wall of the north segment of the Lingding than that in the hanging wall part with a significant western motion. The southwestern coseismic motion observed in the Longitudinal Valley is different from the southeastern coseismic motion near epicentral area predicted according to an oblique-dip faulting. It implies that an unknown west-dipping fault system located on the footwall portion of the Milun and Lingding faults could be also triggered during the 0206 Mw 6.4 offshore Hualien earthquake. The coseismic deformation from D-InSAR of both ascending and descending orbits from ALOS-2 and Sentinel-1 radar images show similar results with our observation from continuous GPS measurements and support the ideas of mutifault ruptures during the 0206 Mw 6.4 offshore Hualien earthquake. It suggests that the 2018 Mw 6.4 Hualien earthquake triggered the multi-fault ruptures of the different fault system, similar to the cases of multiple fault slip triggering during the 2010 Mw 6.2 Jia-Shian earthquake (Lin et al., 2016), the 2016 Mw 6.4 Meinong earthquake occurred in southern Taiwan (Huang et al., 2016; Le Béon et al., 2017) and multi-fault ruptures of the 2016 Mw 7.8 Kaikōura earthquake occurred in New Zealand (Hamling et al., 2017).

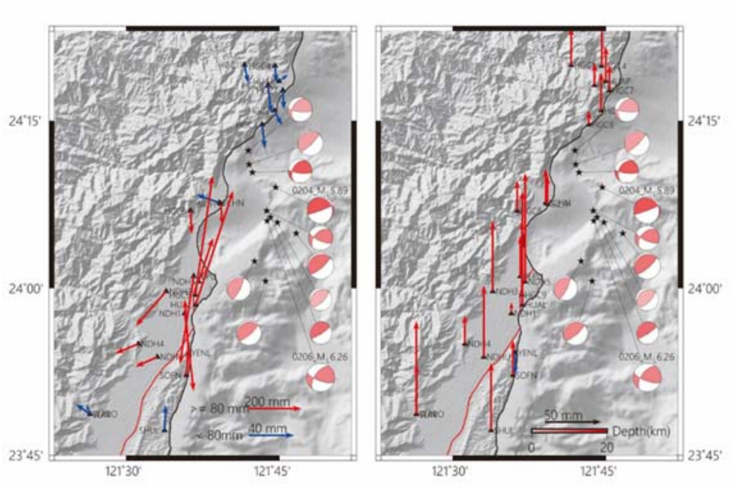

Fig. 1. Coseismic displacement of daily solutions from continuous GPS observed in Mw 6.4 Hualien earthquake. Left figure presents the horizontal displacement and right figure shows the vertical displacement. Focal mechanism are given from BATS.

References

Bonilla, M. G., A review of recently active faults in Taiwan. U. S. Geological Survey Open File Report, 75-41, 58 pp, 1975.

Bonilla, M. G., Summary of Quaternary faulting and elevation changes in Taiwan. Geol. Soc. China Mem., 2, 43-55, 1977.

Hamling, I. J., S. Hreinsdóttir, K. Clark, J. Elliott, C. Liang, E. Fielding, et al., Complex multifault rupture during the 2016 M w 7.8 Kaikōura earthquake, New Zealand. Science, 356(6334), eaam7194, doi: 10.1126/science.aam7194, 2017.

Hsu, M.-T., Seismicity of Taiwan and some related problems. Bull. Intern. Inst. Seismol. Earthq. Eng., 8, 41-160, 1971.

Hsu, T.-L., Recent faulting in the Longitudinal Valley of eastern Taiwan. Geol. Soc. China Mem., 1, 95-102, 1962.

Huang, M.-H., H. Tung, E. Fielding, H.-H. Huang, C. Liang, C. Huang and J.-C. Hu, Multiple fault slip triggered above the 2016 Mw 6.4 MeiNong earthquake in Taiwan. Geophys. Res. Lett., 43, 7459-7467, doi: 10.1002/2016GL069351, 2016.

Le Béon, M., M.-H. Huang, J. Suppe, S.-T. Huang, E. Pathier, W.-J. Huang, C.-L. Chen, B. Fruneau, S. Baize, K.E. Ching and J.-C. Hu, 2017: Shallow geological structures triggered during the Mw 6.4 Meinong earthquake, southwestern Taiwan. Terr. Atmos. Ocean. Sci., 28, 663-680, doi: 10.3319/TAO.2017.03.20.02, 2017.

Lin, K.-C., B. Delouis, J.-C. Hu, J.-M. Nocquet and L. Mozziconacci, Reassessing the complexity of the rupture of the 2010 Jia-Shian Earthquake (Mw 6.2) in Southwestern Taiwan by inverting jointly teleseismic, strong-motion and CGPS data. Tectonophysics, 692, 278-294. doi: 10.1016/j.tecto.2015.09.015, 2016.

Reassess coseismic and postseismic slip on triggered shallow slip of 2016 Mw 6.4 Meinong earthquake by high-rate GPS, campaign GPS, InSAR and strong motion observation

Jyr-Ching Hu*[1], Ying-Hui Yang[1], Hsin Tung[1] and Min-Chien Tsai[3]

1. Department of Geosciences, National Taiwan University, Taipei, Taiwan, R.O.C
2. School of Civil Engineering and Architecture, Southwest Petroleum University, Chengdu, China
3. Seismological Center, Central Weather Bureau, Taipei, Taiwan, R.O.C.

Abnormal high strain accumulation across the fold-and-thrust belt in SW Taiwan are revealed by the Continuous GPS (cGPS) from 2007 – 2015 (Tsai et al., 2017). In general, the high strain rate is accommodated by the major active structures in fold-and-thrust belt of western Foothills. Surprisingly the abnormal high strain rate with significantly uplift rate was observed across the Lungchuan fault in which the aseismic creeping behavior is dominated by the plastic deformation of mudstone in the Gutingkeng formation (Tsai et al., 2017). Furthermore, high Vp/Vs ratio was observed across the epicentral area of 2016 Mw 6.4 Meinong earthquake which imply that high fluid contents in mid-crust to shallow depth could weaken the friction of the major décollement. In addition, high overpressure zone was observed in two wells close to the Lungchuan fault could also support the hypothesis of weakening of the frictional coefficient along the major décollement. According to the distribution of coseismic uplift across the Lungchuan fault to the Tainan Tableland, a clear evidence of multiple fault slips was triggered by the 2016 Mw 6.4 Meinong earthquake at ~15 km (Huang et al., 2016; Le Béon et al., 2017; Tsai et al., 2017). The surface coseismic deformation is mainly controlled by a fault-related folding structures connected to the shallow décollement around 5 - 10 km depth, in which the moderate earthquakes locate in mid-crust could trigger slip along the weak décollement (Huang et al., 2016; Lin et al., 2016).

We use multisource data including the high-rate GPS, static GPS, InSAR and strong motion observations are used to reassess the coseismic and postseismic fault model of multiple fault slip triggered on shallow structure during the 2016 Mw 6.4 Meinong earthquake in Taiwan. The west-dipping Lungchuan backthrust fault and Kuanmiao fault are considered as the triggered by the Meinong main event (Le Béon et al., 2017) which is different from fault model triggered by east-dipping shallow structures proposed by previous study using joint inversion with teleseismic data, InSAR and GPS (Huang et al., 2016). First, the ascending and descending ALOS-2 and Sentinel-1 InSAR observations are jointly used to infer the fault geometry, coseismic and postseismic slip model of the 2016 Meinong earthquake. Then the near-filed static GPS data are used to estimate the coseismic faulting model of this event based on the fault geometry model derived from InSAR data. The GPS-derived faulting model shows that the mainshock results from the rupturing of a point source, and the joint inversion result using the high-rate GPS data and the strong motion data also shows that the significant faulting is only found in the zone around the hypocenter. Lots of postseismic slip has been found both on the main fault and the two shallow faults. In addition, we find that the coseismic rupture of the main fault causes positive Coulomb stress change in the areas with significant postseismic slip on the two shallow faults. It suggests that the two shallow faults could be triggered by the coseismic motion of the main fault, and then results in severe surface motion and seismic hazard in the far-field of the main event.

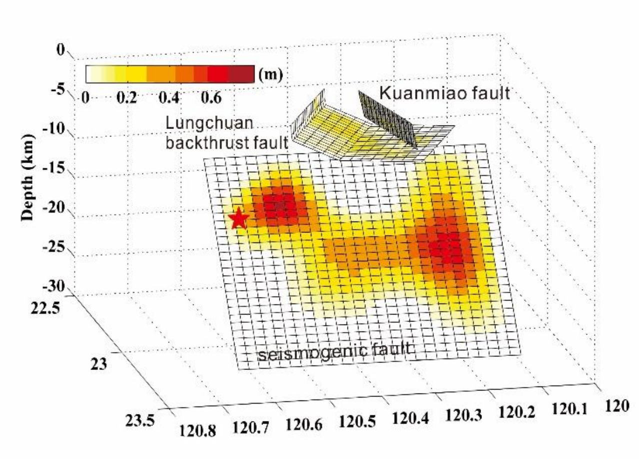

Fig. 1. Inferred multi-fault slip model of 2016 Mw 6.4 Meinong Earthquake from InSAR based on ALOS-2 radar images with both ascending and descending orbits. Red star represents the hypercenter of main shock.

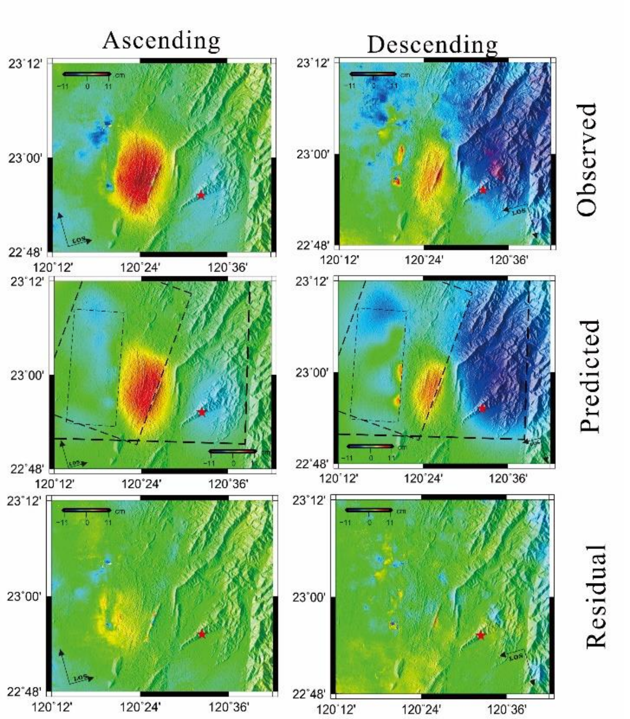

Fig. 2. Comparison of coseismic deformation between the InSAR observation and predicted from multi-fault slip model of 2016 Mw 6.4 Meinong Earthquake from ALOS-2 radar images with both ascending and descending orbits. Red star represents the epicenter of main shock.

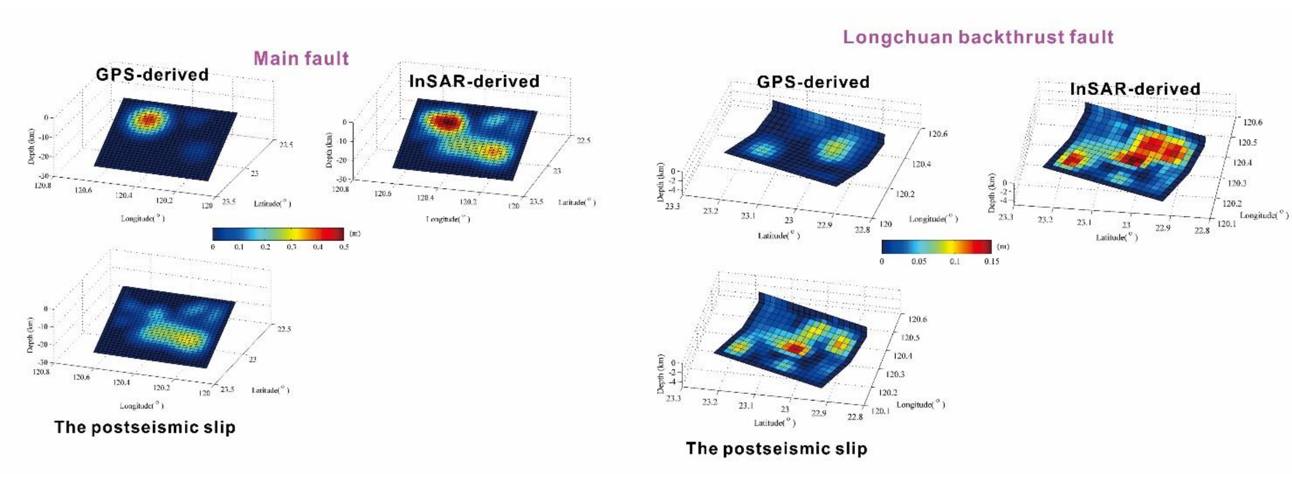

Fig. 3. Inferred of the coseismic and postseismic slip on the main seismogenic fault and triggered Lungchuan backthrust fault by using CGPS and InSAR data, respectively.

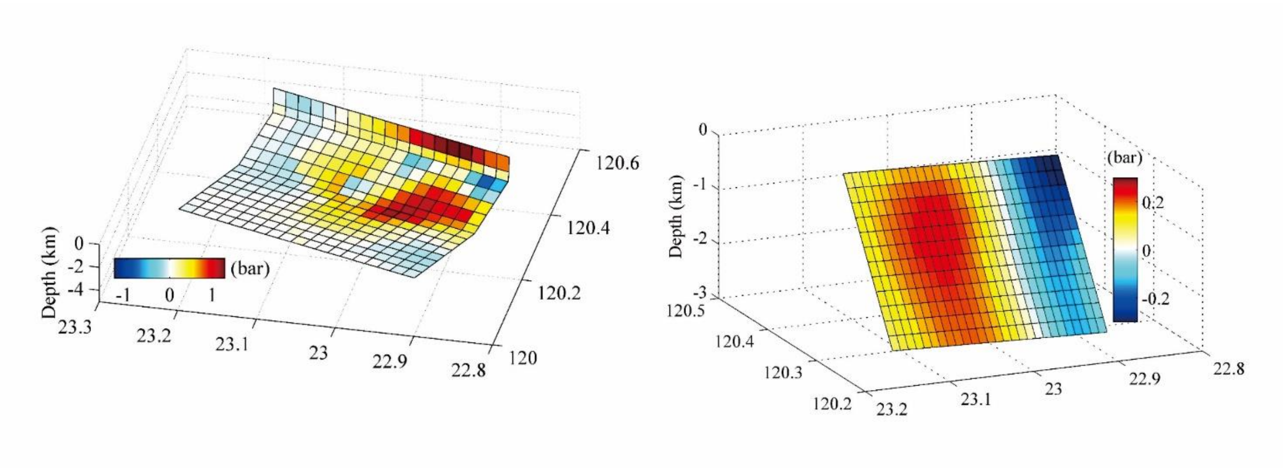

Fig. 4. Coulomb stress changes (CFC) due to the GPS-derived Main seismogenic fault slip. Right panel: CFC along the Lungchuan backthrust fault; left panel: CFC on the Kuanmiao fault.

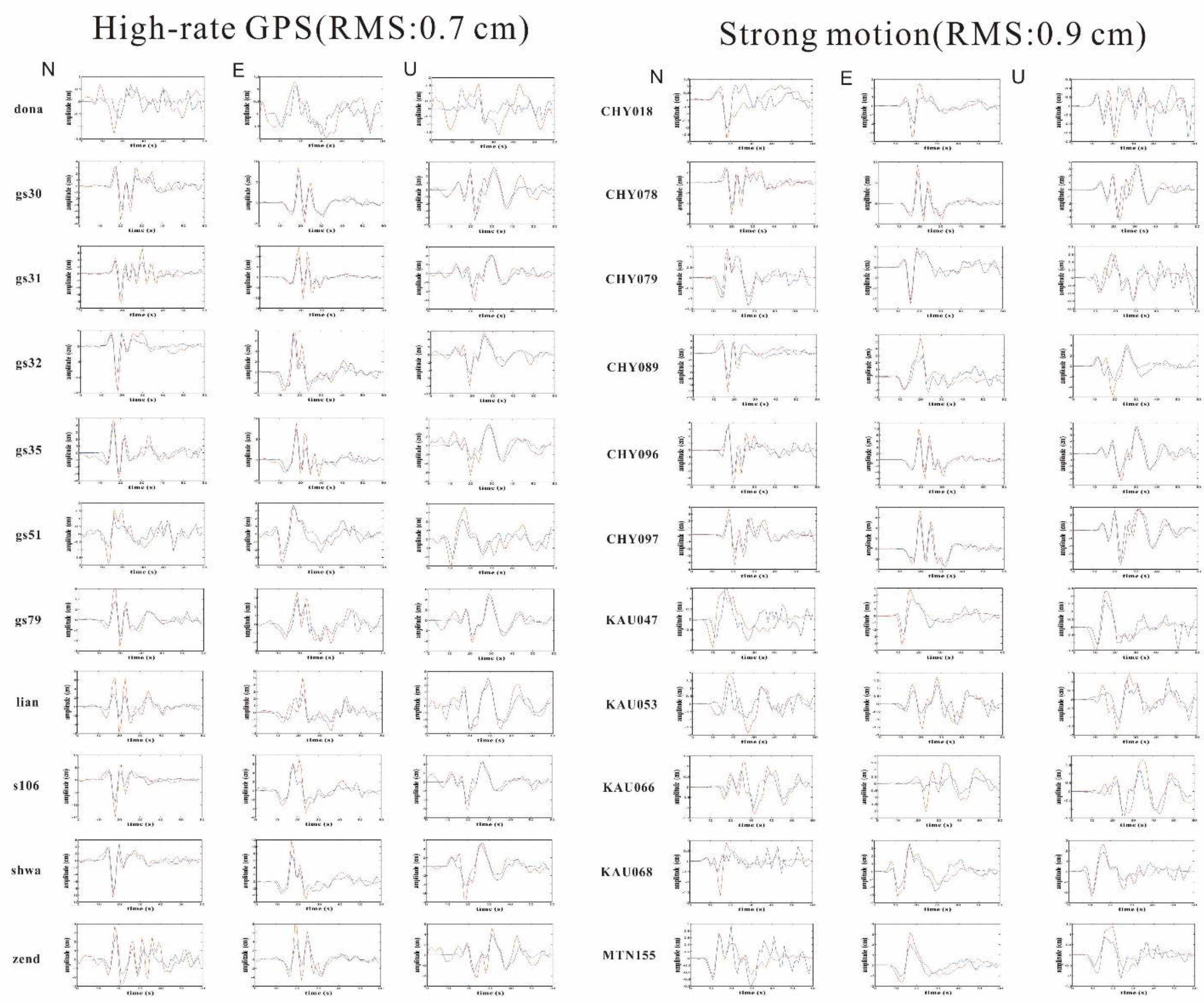

Fig. 5. Waveform fitting of dynamic faulting jointly estimated by high-rate GPS and strong motion data respectively.

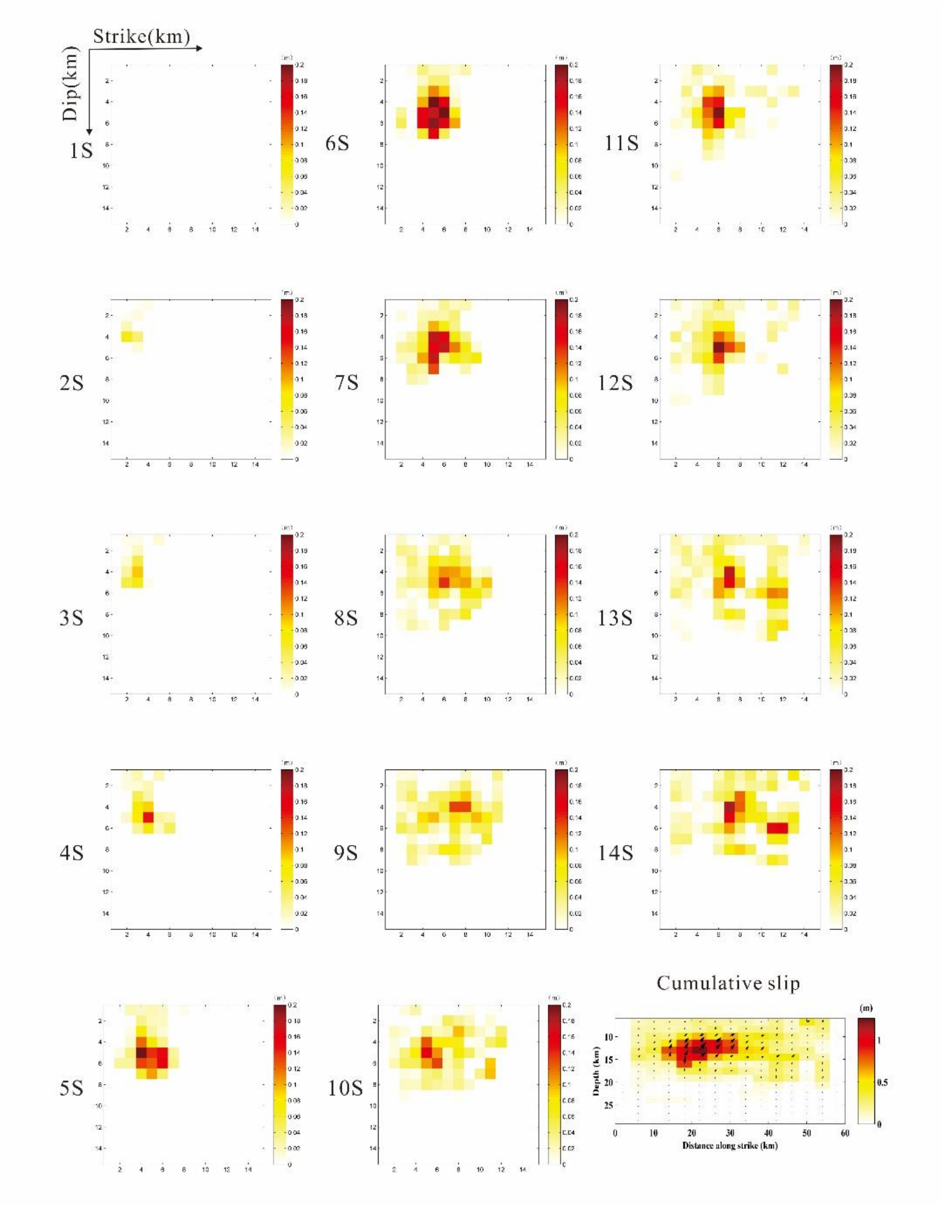

Fig. 6. Dynamic slip distribution and cumulative slip on fault plane jointly estimated by high-rate GPS and strong motion data respectively.

References

Huang, M.-H., H. Tung, E. Fielding, H.-H. Huang, C. Liang, C. Huang and J.-C. Hu, Multiple fault slip triggered above the 2016 Mw 6.4 MeiNong earthquake in Taiwan. Geophys. Res. Lett., 43, 7459-7467, doi: 10.1002/2016GL069351, 2016.

Le Béon, M., M.-H. Huang, J. Suppe, S.-T. Huang, E. Pathier, W.-J. Huang, C.-L. Chen, B. Fruneau, S. Baize, K.E. Ching and J.-C. Hu, 2017: Shallow geological structures triggered during the Mw 6.4 Meinong earthquake, southwestern Taiwan. Terr. Atmos. Ocean. Sci., 28(5), 663-680, doi: 10.3319/TAO.2017.03.20.02, 2017.

Lin, K.-C., B. Delouis, J.-C. Hu, J.-M. Nocquet and L. Mozziconacci, Reassessing the complexity of the rupture of the 2010 Jia-Shian Earthquake (Mw 6.2) in Southwestern Taiwan by inverting jointly teleseismic, strong-motion and CGPS data. *Tectonophysics*, **692**, 278-294. doi: 10.1016/j.tecto.2015.09.015, 2016.

Tsai, M.-C., T.-C. Shin and K.-W. Kuo, Pre-seismic strain anomalies and coseismic deformation of Meinong earthquake from continuous GPS. Terr. Atmos. Ocean. Sci., 28(5), 1-23, doi: 10.3319/TAO.2017.04.19.01.

Vertical deformation of the 2017 M5.6 earthquake detected by precise leveling in the Ontake earthquake swarm area, central Japan

Masayuki MURASE1, Fumiaki KIMATA[2], Yoshiko YAMANAKA[3], Takeshi MATSUSHIMA[4], Takahiro KUNITOMO[3], Hitoshi MORI[1], Yang LI[1], Takamasa HASE[1], Kazuki Ofuchi[1], Yuta Maeda[3], Shinichiro Horikawa[3], Takashi Okuda[3], Kenjoro MATSUHIRO[3], Kazushi TANOUE[3], Kazunari Uchida[4], Yoshiko TEGURI[4], Rintaro MIYAMACHI[4], Kaori MORITA[4], Shin Yoshikawa[5], Hiroyuki INOUE[5], Hiroaki YANAGISAWA[6], Tomoyuki MATSUMURA[6], Takafumi TANIGUCHI[6], Isao KAGEYAMA[6], Syuichi HOSODA[6], Takahiro YANADA[6]

1.Nihon University, 2.Tono Research Institute of Earthquake Science, ADEP, 3.Nagoya University, 4. Kyushu University, 5.Kyoto University, 6.Japan Meteorological Agency

The M5.6 earthquake occurred in the eastern flank of the Ontake volcano in June 25, 2017. We conducted the precise leveling surveys in the eastern flank of the Ontake volcano in April 2017, September 2017, and April 2018, and discussed vertical deformations related to this M5.6 earthquake.

The swarm activity is continued in the southern and eastern flanks of the Ontake volcano since 1976 (Yamazaki, 2008). In order to detect the deformation related to the swarm activity, we have conducted the precise leveling surveys in the eastern flank of the Ontake volcano from 2002 (Kimata et al., 2004). The leveling routes of about 38 km with 98 benchmarks were established on the eastern flank of Mount Ontake volcano. The main routes were extended to the Yashikino village (Kakehashi and Yashikino routes). In order to improve the spatial layout of the benchmarks, a branched leveling routes were established (Kiso-Onsen, Ontake Ropeway and Nakanoyu routes).

In April 2017 (before the earthquake), all leveling routes were observed. The M5.6 earthquake occurred just beneath the Yashikino and Kiso-Onsen leveling routes in June 25, 2017. In order to detect the vertical deformation associated with this earthquake, the urgent leveling survey was conducted in the Yashikino and Kiso-Onsen routes in September 2017. The benchmarks of the Yashikino and Kiso-Onsen routes showed uplift in the period from April to September 2017. The maximum uplift of 28mm was detected in central part of Yashikino route.

In April 2018, we conducted the leveling of all leveling route, and detect the deformation after the earthquake. The benchmarks of the Yashikino and Kiso-Onsen routes also showed uplift in the period from September 2017 to April 2018. The maximum uplift of 5mm was detected in central part of Yashikino route.

We need continued and careful observation of the deformation in the eastern flank of the Ontake volcano.

Reference

Kimata, F., R. Miyajima, M. Murase, D. Darwaman, T. Ito, Y. Ohta, M. Irwan, K. Takano, F. Ibrahim, E. Koyama, H. Tsuji, T. Takayama, K. Uchida, J. Okada, D. Solim, and H. Anderson, Ground uplift detected by precise leveling in the Ontake earthquake swarm area, central Japan in 2002-2004, Earth Planets Space, 56, e45-e48, 2004.

Yamazaki, F., The volcanic activity and swarm activity in the ontake volcanic area, Report of Tono research institute of earthquake science, 21, 111-124, 2008.

Eruptions and earthquakes in the Hawaii Island

Yuzo Ishikawa (GSJ, AIST)

M6.9 earthquake occurred on May 4 at the southeast coast of the Hawaii island (right top figure). In the East Rift Zoon(ERZ) of the Hawaii island, magma overflowed at many fissures from May 3. The explosive eruption with M5.3 earthquake was occurred at the summit of the Mt. Kilauea on May 17. After this event, there were 53 explosive earthquakes of which magnitude were bigger than 5 until Aug. 2. The interval of these earthquake occurrence were from 20 hours to 53 hours. The magnitudes were from 5.0 to 5.4 and these events are all normal faulting. After M5 earthquake occurrence, there were calm for a few hours and next, small earthquakes gradually occurred. The number of earthquakes gradually increased and the size of magnitude also increased. It is the similar pattern to the recurrence of inter-plate great earthquake. So, these seismic and geodetic data are very important for the earthquake prediction.

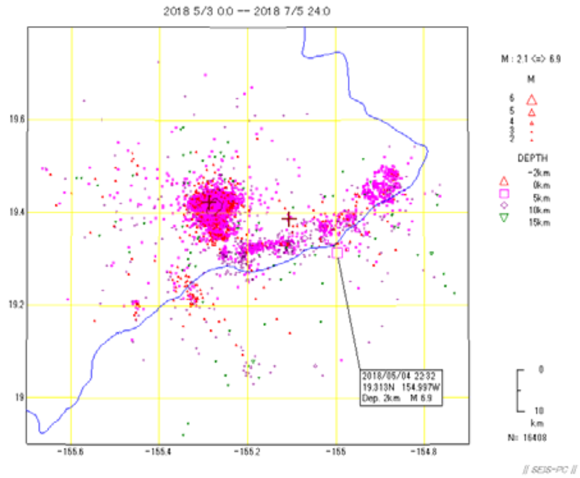

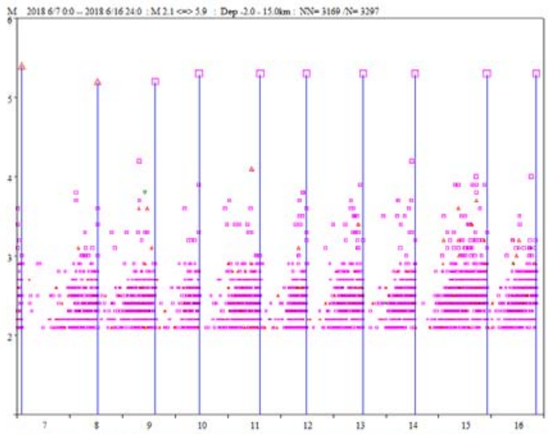

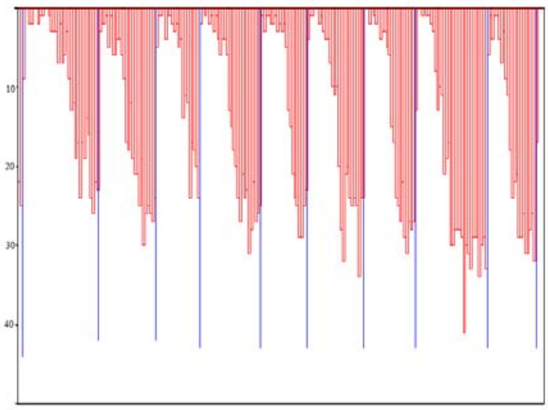

Figure captions

Top: Sesimicity map in Hawaii island. The main shock (M6.9) was shown parameter. Two pluses show the volcanoes of Kilauea and Pu'u'o'o.

Middle: The magnitude-time figure in and around Kilauea crater for June 7 to 16. The blue lines are the M5 events.

Bottom: The daily number-time figure an and around Kilauea crater for June 7 to 16.

Case studies of long- and short-term injection-induced earthquakes

Xinglin Lei

Geological Survey of Japan, AIST

Enhanced geothermal systems (EGSs), shale gas fracking, and geological sequestration of CO_2 and other waste fluids play an important role in the mitigation of global warming. In these applications, fluids are intensively pressed into deep formations or reservoirs. Fluid-injection-induced earthquakes have attracted growing attention and must be adequately addressed in order for these applications to be operated efficiently and safely. In the present study, we describe several case studies of injection-induced seismic activity in a relatively aseismic region in the southwestern Sichuan Basin. In previous decades, a number of seismic sequences with sizable earthquakes in the range of M4 to M5 have been observed (Lei et al., 2017; Lei et al., 2013; Lei et al., 2008). Their timings, locations, and occurrence patterns in statistical models suggest that these sequences were induced by water injection in deep wells for various purposes, including wastewater disposal, production of well salt, and hydrofracturing of shale gas. Event rates fluctuated following changes in injection rates and tapered off after injection ceased. Most events exhibit shear fracturing mechanisms, which, together with hypocenter location data, demonstrates that pre-existing faults, known or unknown, in sedimentary formations have a governing role in controlling the hypocenter distribution of induced earthquakes. Faults on a relatively larger scale act as a bounding interface for horizontal fluid flow and as a leakage path for vertical fluid flow. Statistical analysis has revealed that these sequences are more swarm-like, demonstrating significantly lower Omori-law aftershock productivity as compared with tectonic earthquakes. During earlier stages of the injections, the total fraction of seismically triggering earthquakes is 40% to 60%, while the forced earthquake rate increases with injection time, indicating that the stress in the formations is originally critical or subcritical. In later stages, the total fraction of forced (by injection-induced stresses) seismicity may be approximately 90%. The mechanism solution of large events indicates that an inhomogeneous stress field on the reservoir scale or overpressure of fluid is required to interpret the reactivation of badly oriented faults.

Motivated by the desire to better understand the mechanism of damaging events so that they can be avoided or mitigated, we also started laboratory rock fracture experiments using an acoustic emission technique. We systematically carried out rock fracture tests using samples of typical sedimentary rocks collected from sites of injection-induced seismic swarms. Since most injection-induced earthquakes are located in sedimentary strata of a wide range of lithology and depth, the fracture behaviors of such rocks are important. The obtained results indicate that the pre-Triassic rocks in the Sichuan Basin, including dolomite or dolomitic limestone and shale, are strong and demonstrate brittle fracturing behaviors. Such properties are necessary in order to maintain a high level of reservoir stress and the resulting seismic fracturing. The insights gained from the proposed multi-scale approaches provide a better understanding of why damaging events occur, so that they can be avoided or mitigated.

Lei, X., Huang, D., Su, J., Jiang, G., Wang, X., Wang, H., Guo, X., Fu, H., 2017. Fault reactivation and earthquakes with magnitudes of up to Mw4. 7 induced by shale-gas hydraulic fracturing in Sichuan Basin, China. Scientific Reports 7, 7971.

Lei, X., Ma, S., Chen, W., Pang, C., Zeng, J., Jiang, B., 2013. A detailed view of the injection-induced seismicity in a natural gas reservoir in Zigong, southwestern Sichuan Basin, China. Journal of Geophysical Research: Solid Earth 118, 4296-4311.

Lei, X., Yu, G., Ma, S., Wen, X., Wang, Q., 2008. Earthquakes induced by water injection at ~3 km depth within the Rongchang gas field, Chongqing, China. Journal of Geophysical Research 113.

Geochemical variability of deep seated fluid along median tectonic line

Hitomi Nakamura
(Geological Survey of Japan, AIST)

Deep seated brine has been identified as a spring water upwelling in non-volcanic region in Japan. They have distinct chemical signatures such as a high-chlorine content, O-H isotopic ratios departing from the meteoric water line with no tritium, and a high 3He/4He ratio indicating a deep-origin (Matsubaya et al., 1973; Tanaka et al., 1984; Masuda et al., 1985). In addition to these geochemical characters, recent studies suggest a linkage with the slab-derived fluid, based on unconventional isotopes and elements for studies on spring waters, such as Nd and Pb isotopes and Rare earth elements (REEs) (e.g., Kazahaya et al., 2014; Kusuda et al., 2014; Nakamura et al., 2014; 2015). The geochemical behaviour and partitioning of REEs between solid and fluid are sensitive to temperature, volatile fugacity, and pH during the upwelling processes where these parameters are potentially variable (Ohta and Kawabe, 2000). By using this sensitivity of REEs in spring waters, we have investigated the origin and upwelling processes of the deep-seated fluids along the Median Tectonic Line (MTL) in central to southwest Japan (Nakamura et al., 2016; this study).

Using Earthquake induced Post-seismic Recovery of Groundwater Variations to Estimate the Hydraulic Properties of Aquitards

Shih-Jung WANG [#+], Wen-Chi LAI[*], Kuo-Chin HSU[*], Chein-Lee WANG[*], and Liang-Tzu HSU[*]

National Central University, Taiwan

**National Cheng Kung University, Taiwan*

[#]*Corresponding author: sjwang1230@gmail.com* [+]*Presenter*

Earthquake-induced crust stress (strain) triggers groundwater level variations over a short period of time in a large area. These groundwater anomalies can be used to investigate aquifer systems. This study uses a poroelastic model to fit the post-seismic variations of groundwater level triggered by the Chi-Chi earthquake to evaluate the hydraulic properties of aquitards in the Jhoushuei River alluvial fan (JRAF), Taiwan. Six of the adopted eight wells with depths of 70-130 m showed good agreement with the recovery theory. The mean hydraulic conductivities (K) of the aquifers for the eight wells are 1.62×10^{-4}-9.06×10^{-4} m/s, and the thicknesses are 18.8-46.1 m. The thicknesses of the aquitards are 11.3-42.0 m. Under the isotropic assumption for K, the estimated values of K for the aquitards are 3.0×10^{-8}-2.1×10^{-6} m/s, corresponding to a silty medium. The results match the values obtained for the geological material of the drilling core and those reported in previous studies. The estimated values were combined with those given in previous studies to determine the distribution of K in the first two aquitards in the JRAF. The distribution patterns of the aquitards reflect the sedimentary environments and fit the geological material. The proposed technique can be used to evaluate the K value of aquitards using inverse methods. The inversion results can be used in hydrogeological analyses, contaminant modeling, and subsidence evaluation.

Announcement: The content of this study is from the paper published in *Groundwater* as: Wang, S.-J.*, K.-C. Hsu, C.-L. Wang, W.-C. Lai, and L.-T. Hsu, 2017, Evaluation of Hydraulic Properties of Aquitards Using Earthquake-Triggered Groundwater Variation, *Groundwater*, 55(5), 747-756.

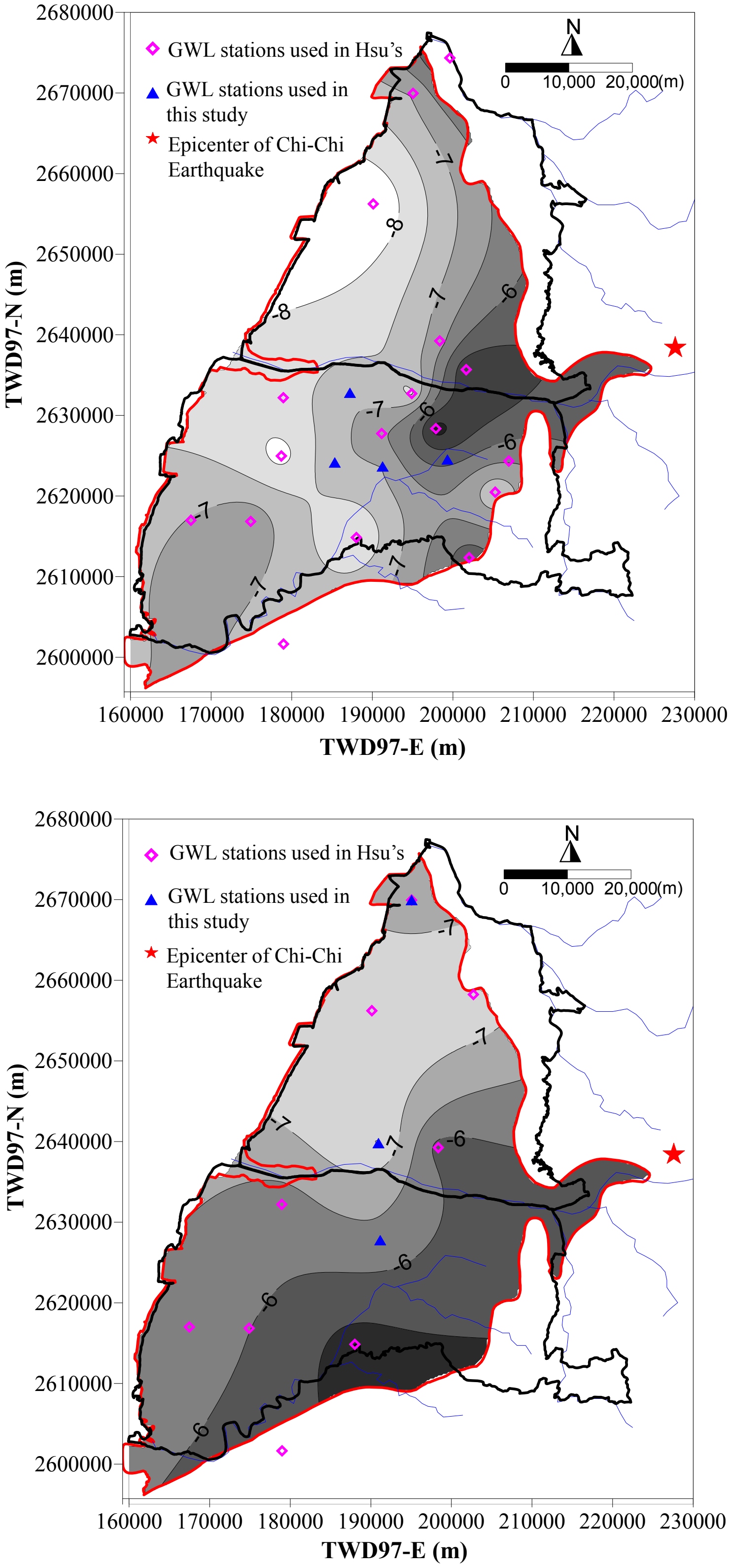

Figure 1. Distribution of hydraulic conductivity in aquitard 1 and aquitard 2 obtained by combining results of this study and a previous study. Contour values are log10K (GWL: groundwater level).

Comparison of Permeability of Fault Zone Between In-situ Hydraulic Tests and Laboratory-Derived Data at the Median Tectonic Line, Central Japan

Norio Matsumoto[1] and Norio Shigematsu[1]

[1] Geological Survey of Japan, AIST

The permeability structure around fault zones plays an important role in fault hydrogeology and movement. A number of studies about laboratory measurements of permeability of natural and synthetic fault materials indicate low permeability within the fault core and variable permeability in the complex damage zone structure, which is governed by macroscale fracture networks and low-permeability deformation bands.

Wibberley and Shimamoto (2003) reported laboratory-derived permeability data for the Median Tectonic Line (MTL) fault zone using samples from the Tsukide outcrop. Their permeability data show wide variation with fault rock microstructure, and central slip zone gouges have the lowest permeability.

The Geological Survey of Japan, AIST has drilled three boreholes into the MTL at the Matsusaka-Iitaka (ITA) observatory about 15 km east of the Tsukide outcrop. We studied the fault zone permeability in two of these boreholes using hydraulic tests and groundwater-pressure observations and also measured the permeability of drillcore samples of protoliths. Hole 1 (total depth 600m) was penetrated the Median Tectonic Line (MTL) at a depth of 473.9m. Total depth of Hole 2 is 208m. We obtained core samples and well logging data and conducted hydraulic tests in these wells. Screened depth of Hole 1 is 547.6-558.5 m and is located in the lower fracture zone of the MTL fault zone developed in the Sanbagawa metamorphic rocks. Screened depth of Hole 2 is 145.5-156.4 m and is located at a branch fault in the Ryoke granitolds (Shigematsu et al., 2012).

Our aim is to verify the complex permeability structure at the MTL showed by Wibberley and Shimamoto (2003) by using in-situ permeability data produced by hydraulic tests and long-term groundwater-pressure observations.

We performed hydraulic tests and long-term groundwater-level observations at Holes 1 and 2 drilled into a major strand of the MTL fault zone and one of the branching faults in the hanging wall of the MTL, respectively. The estimated permeabilities ranged from 5.3×10^{-17} to 5.0×10^{-16} m^2 and 4.4×10^{-16} to 1.5×10^{-15} m^2 at Holes 1 and 2, respectively. Moreover, recovery rates of long-term background water level in Holes 1 and 2 suggest the presence of zone adjacent to the aquifer with lower permeability than that estimated by the hydraulic tests. The bulk permeability values we obtained were similar to those obtained from MTL outcrop samples at confining pressure of 50MPa by Wibberley and Shimamoto (2003). The variability in permeability found in this study reflects the complex structure of the MTL fault zone.

Statistical Evaluation of Precursory Phenomena – A Review.

Masao Nakatani[1]
[1]Earthquake Research Institute, The Univ. of Tokyo, Japan

One-on-One Claim of Earthquake Precursor

When we find a (big) earthquake was preceded by something unusual (let's call it *anomaly*), it is natural to suspect that the anomaly was a precursor of the earthquake. However, unless a persuasive mechanism is shown to explain why the earthquake occurred (shortly) after the appearance of the anomaly, it is virtually impossible to believe that the anomaly was a precursor, that is, it appeared for a reason that an earthquake was about to occur. One can always say that it *could be* a precursor, but just accumulating hundreds of 'could-be' cases does not take us anywhere. Even multi-parameter studies do not improve the situation fundamentally. We may be convinced of the occurrence of some event in the crust, or even what it was, but the real hard part is being convinced that *the* event was related to the occurrence of the earthquake that followed, to which simultaneous appearance in multiple parameters is of little help.

In my opinion, the only precursor convincing, on a one-on-one basis, is the huge fault slip that quickly loads up the locked part of the fault that will dynamically slip in the earthquake that follows. Although such is often invoked as a mechanism of various claimed precursors, note that a huge slip in the crust should be resolved by geodetic observation. The same criticism applies to the often hypothesized rapid stress increase over the source region of the coming earthquake, which would be detected geodetically as well. Unless accompanied by large geodetic changes, only small precursory changes are allowed for stress/deformation, even as a speculation, which would have only small impacts on the occurrence of the earthquake, and hence relevance to the earthquake that followed remains 'could be' because the earthquake could happen without such small events just by waiting for some more tectonic loading. Also, it is clear that small increment of stress leads to an earthquake only when the stress has been already very close to the strength. Therefore, those small incidents can occur many times, most of them not followed by an earthquake. When it occurred at the right timing, yes, it was really a precursor, but how can we believe that the particular small crustal incident that preceded an earthquake was the precursor when we do not know the stress was already very close to the failure strength? This is a fundamental difficulty in proving the existence of precursor on a one-on-one basis.

Some classic, ideal precursor scenarios where precursors indicate that the fault is at the verge of dynamic instability, including the dilatancy [e.g., Scholz et al., 1973] and the preslip-nucleation [e.g., Tse and Rice, 1986] theories, do not suffer the above difficulty because necessity of those processes is built in. However, observation has shown those expected precursors rarely appears, betraying its built-in premise of inevitability. These days, the failure of these scenarios has been ascribed to the fact that the initiation of instability does not control how far it will grow, as improved observation of dynamic earthquake rupture processes provides more support for the view that earthquakes grow by cascading up through hierarchical heterogeneity of faults [Ide and Aochi, 2005]. Expected precursors may sometimes occur [Noda et al., 2013], but as long as it is a rare case, it is difficult to make precursor proof on individual cases.

Statistical Claim of Earthquake Precursor

Nevertheless, it is not difficult to prove the existence of precursors, long-term or short-term, once we give up the one-on-one approach trying to prove for individual cases. Instead, we can check for the *existence of tendency* that earthquakes occur at a higher probability following the appearance of certain type of anomaly.

People often try to achieve this objective on cross table, counting anomalies that were followed by earthquakes and were not. However, this is a bad idea. Anomalies often appear intermittently in a period shorter than the typical lead time of the precursor. So, anomaly count, and in turn the evaluation result from the cross table depends badly on how one parses the observed time-series data into countable anomalies. The parsing should be done so that anomalies related to one earthquake collectively make one count, but this is usually impossible without knowing the actual time and location of the earthquake. As a result, people look for different parsing rules for different earthquakes retrospectively, that is, make excuses and lose credence.

A practical, robust, EASY, and well-founded alternative method to prove the existence of precursor tendency is to make and evaluate trial (retrospective) forecasts based on the anomalies. In this method, instead of counting anomalies, we measure the volume of the alarmed space-time [Zechar and Jordan, 2008], which makes our life incredibly easy. Forecasts can be made by any procedure as long as it can be objectively stated and not using the information not existing before the earthquake. Recognition of anomalies is only an internal step and not a must; evaluation is solely made against forecasts, by comparison with the actual occurrences of earthquakes. Hence, forecasts need to specify the range of location, time, and the magnitude of the earthquake to expect.

Figure 1 illustrates the method. Forecasts were made by probably the simplest procedure. If an anomaly appears at a point, then the area of spatial extent *R* around is declared 'alarm ON' for a duration *T*. Do that every time an anomaly appears. The eventual alarmed space-time (painted red) becomes the logical sum of the *RT* zones turned on by each anomaly. Missing observation (black) is not a problem. The space-time volume for which alarm state cannot be decided (gray) is excluded from evaluation as undecidable volume. Note that the undecidable volume extends beyond the no-observation volume because we cannot be sure of whether an anomaly appeared within *RT*, except when an anomaly already appears after the observation resumes (the red zone overlapping the gray zone). In other words, the alarm-OFF zone (pink) is the space-time volume where we know that anomalies did not appear in the past *RT*, and earthquakes occurred there is a surprise (a.k.a missed) earthquake.

The Figure 1 procedure handles the situation of clustering anomalies, as exemplified by the three anomalies near the center of the figure. Few people would complain on the resultant red zone, I hope.

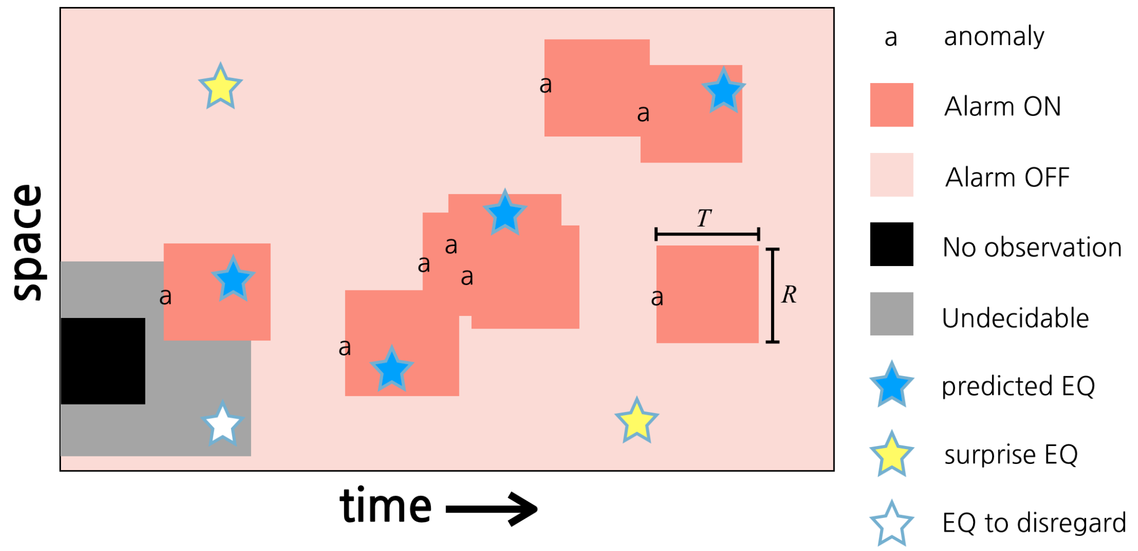

Figure 1. Anomalies, Alarms, and Earthquakes.

You may devise whatever elaborate forecast procedures unleashing your experience and speculations. For example, you may want to set R and T according to the details of the observed anomaly. For example, if you think that earthquakes tend to occur only some time after your anomaly appear, you may wait for some time before turning on alarm after seeing the anomaly. By converting anomalies into forecasts, your subjectively speculated 'tendency' becomes an objectively testable proposition. In retrospective testing, there's always the possibility of over-optimization. Forecasting is a modeling, so there would be a way to penalize overly complicated procedures. But, in my experience, making an algorithm to achieve Gerrymander forecasts is very difficult, when there are, say, more than 7 earthquakes to predict. Also, let's not forget that people have common sense.

Evaluation is done by looking at the percentage of earthquakes that occurred in the alarmed volume. This percentage, Anomaly Appearance Rate (AAR), is also known as the Prediction Rate or Alarm Rate, and is same as 1−Miss Rate. The expected value of AAR under the null hypothesis that is none of your anomalies were relevant to the occurrence of earthquakes that followed is equal to the Alarm Fraction (AF), the percentage of alarmed volume against the total volume excepting the undecidable volume. If AAR is significantly higher than AF, we can believe that some of the anomalies that preceded earthquakes were precursors. 'Significant or not' is judged by the p-value, which is the binomial probability that greater or equal number of earthquakes than actual occurs within the alarmed volume by chance. So, even weak tendency can be proven if many earthquakes are available for evaluation. The strength of the precursor tendency is expressed by the ratio AAR/AF, called Probability Gain (PG).

According to the procedure explained above, PG is an improvement of AAR from random forecasting. However, simple calculus shows that the expected earthquake occurrence rate λ (probability of earthquake occurrence per unit space-time volume) is increased by a factor of PG from the base rate λ_0, the λ averaged over the entire space time excepting the undecidable volume. The probability Q_{ON} that an earthquake occurs in the typical alarmed volume of RT (I'm doing this for people who are too used to *counting* anomalies or alarms) is called Success Rate, a.k.a. Hit Rate or 1−False Positive Rate. Q_{ON} is ~ $RT\lambda_{ON}$, where $\lambda_{ON} = PG \times \lambda_0$ is the λ in the alarmed volume. Noticing that Q_{ON} under the null hypothesis is $RT\lambda_0$, we can see that the success rate is also improved by the dame factor PG from that by random forecasting.

It is very important to understand the exact proposition of the statistical claim. As understood from the null hypothesis state earlier, the proposition is that s*ome of* the anomalies that (shortly) preceded the earthquake were really precursors. So, pro-precursor people should not forget that some of the same-looking anomalies that did precede earthquakes were actually just irrelevant anomalies that happened to occur in such a misleading space time. We cannot tell which one was precursor and which one was not, but we can tell the real percentage of earthquakes that were preceded by precursors is ~ $AAR-AF$, which I would call the net-AAR. On the other hand, anti-precursor people must understand that the statistical claim cannot be falsified by just finding some of the anomalies that preceded earthquakes were actually irrelevant signals. The statistical claim has drawn conclusions with those factors considered.

Preparation Process and Precursor (PPAP).

In the presentation, I will review results of statistical evaluation. There are quite a few proven precursory phenomena. PG distributes widely from ~2 to a few tens of thousand. All the forecasts utilizing short-term foreshock activities have $PG > 100$, while PG of all the others are < 20 [Nakatani, 2018]. While foreshocks provide a great predictive power, we must also note that much of its predictive power seems to derive from the mechanism of aftershock triggering, not requiring any physical preparation process [Helmstetter et al., 2003] such as the fault at the verge of failure or critically organized state that allows once started rupture grows easily without arrested in the middle. This shocking paper demonstrates that even the trivial-sounding notion that precursors must be signs of some preparation process altering the physical state of the crust is, in fact, too naive a presumption as pointed out by Tsumura [1994].

Acknowledgements

Supported by MEXT's Earthquake and Volcano Hazards Observation and Research Program

Connection between historical earthquake and groundwater anomaly

Yasuyuki Kano[1]

[1] Earthquake Research Institute, The University of Tokyo, Japan

Ground water anomalies are documented in historical sources. For example, it is well known that hot spring in Kii Peninsula and Shikoku Island, southwestern Japan repeatedly showed anomalous changes at the time of large earthquakes occurred at Nankai trough. From the observation of change in well water level we can extract information of strain change associated with earthquakes. Coseismic deformations produce volumetric strain change of crust. The spatial distribution of the strain change can be used to constrain geometry of the source fault. Poroelastic theory and modern borehole observations show that volumetric contraction or extension of 0.1 to microstrain yield 10 cm to 1 m increase or decrease. Although small strain changes cannot be sensed or observed by people, the mechanical coupling between rock and water brings observable change in groundwater. The observable groundwater anomaly produced by natural amplification of crustal deformation is a key to connect historical earthquake study with earthquake hydrology.

Japanese historical earthquake documents show, for example, that well water level change was observed at the time of the 1703 Kanto and 1855 Hietsu earthquake. The source area of the 1703 Kanto earthquake is estimated to be off Boso peninsula, Japan. A well became empty at a village near southern end of the peninsula, which may be caused by ground water level drop associated with volume extension of the crust. Another well locates in middle of the peninsula showed no change, which may be attributed to smaller strain change. The spatial distribution is consistent with coseismic deformation predicted from a source model constrained by geographical examination. The source fault of the 1855 Hietsu earthquake is located at the Atotsugawa fault, central Japan. Decreases in well water were observed at a village close to Toyama bay, which may be attributed to volumetric extension. The location of the village is close to node of four quadrant pattern of volumetric strain predicted from geometry of active fault trace and distributions of damages of houses at the time of the earthquake. The observed decrease well water level and volumetric extension can be used to constrain the fault geometry more accurately.

Observation of Water in Wariishi Hot Spring

Taku Nakamura[1], Shigeki Tasaka[1], Masaya Matsubara[1], and Norio Matsumoto[2]

[1] Gifu University

[2] Geological Survey of Japan, AIST

In this study, we report on the results of the spring water observation at the Wariishi hot spring in Hida City, Gifu Prefecture, and the measurement of the concentration of radioactive radon in the Kamioka mine located in the same area. The Wariishi hot spring is located 2.6 km south of the Atotsugawa fault and is a self-sprinkling sulfur spring with water temperature of 45 ° C, radon concentration of 2.6 ± 0.2 Bq/L, flow rate of 25L/ min. Observations at the Wariishi hot spring have been conducted for over 40 years since 1976, and Gifu University started measuring with an electromagnetic flowmeter since 1998. Since 2004 we have monitored water with 1 Hz data.

It is known that the Wariishi hot spring is a geyser and its cycle varies with increasing and decreasing amount of water. At the occurrence of the earthquakes, fluctuations in the amount of water and the period of the geyser are observed. In the Hida Earthquake on February 27, 2011, the amount of water increased from 27.8 L/ min to 44.8L/min, and in the Tohoku region Pacific offshore earthquake of March 11, 2011 it increased from 44.8L/min to 59.5L/min. An increase in the amount of water or variation of water was observed in all 39 earthquakes with a magnitude of 6.7 or more from August 2004 to December 2017. It was revealed that the period of the geyser is decreasing in nine earthquakes from October 2005 to December 2017.

The concentration of radon gas in the water from the fault of the Kamioka mine, about 10 km northeast of the Wariishi hot spring, has been measured. Measurement is carried out by two methods: continuous measurement of daughter nuclides of radioactive radon by electrostatic collection method and measurement of sampled water with a liquid scintillation counter. The observation point is about 3 km from the entrance to Mozumi gallery, 1000 m underground of the Mt.Ikenoyama. In the liquid scintillation method, fault water flowing through the pit is measured at 5 fixed points for 300m from the upstream to the downstream.

In the measurements from 2017 to 2018, the radon concentration is decreasing while flowing through the pit with the upper stream at 18.4 ± 0.2 Bq/L and the downstream at 2.3 ± 0.1 Bq/L, 300 m. The seasonal fluctuation have not been observed. Radon released from the water into the atmosphere will raise the radon concentration of the air in the pit. On the other hand, seasonal fluctuations are observed in the atmospheric radon concentration due to the atmospheric flow inside the pit.

The earthquake related water level increase at Oi well in Kanagawa prefecture

Yang Li[1], Kazuhiro Itadera[2], Masatake Harada[2] ,Motoo Ukawa[1]

1 Nihon University,　2 Hot Spring Research Institute of Kanagawa Prefecture

The Oi well is one of the observation wells to monitor the groundwater level changes operated by the Hot Spring Research Institute of Kanagawa Prefecture(HSRI). The well is located in the western part of Kanagawa Prefecture near the Kozu-Matsuda fault. The depth of the well is 300 m, the depth of screen is 270～300 m. The permeability of the aquifer is $5.5 \times 10^{-4} cm/s$, and the storage coefficient is 3×10^{-8}(Yokoyama et al. 1995).

The water level is recorded by pressure water level gauge with 1Hz sampling rate. The period we analyzed is from January 2011 to April 2016. In this period 10 earthquakes caused the water level changes more than 5 cm. Except for the 2011 Great Tohoku Earthquake, which exhibited water level decrease, the nine earthquakes show the water level increase after seismic wave arrives.

In our preliminary research, we found that the water level changes after earthquakes in Oi well can be approximated by exponential decay curves expressed as a function: $\boldsymbol{H(t) = a(1 - e^{-bt})}$. In this function, the inverse number of parameter $\boldsymbol{b}$ is a time constant. In Oi well the time constant is in the range of 100~400 s.

We build a　physical model to explain these water increase in Oi well on bases of slug test model. We assume that the aquifer is composed of groundwater (liquid phase) and soil particle (solid phase). The solid phase works as skeleton to support the stratum above the aquifer. Groundwater fill up the void of the skeleton. The solid phase become weak by seismic waves. The part of lithostatic pressure supported by groundwater increase then the water level in Oi well increase.

This model is a reverse process of a slug test, or same as a bailer test. We use the solutions of slug test proposed by Karasaki et al.(1988) to model the water level changes after the earthquake. The solution for the change in water level for a finite radius well subjected to a slug test in a homogeneous medium is the best fit to the water level changes in Oi well.

The present analysis indicates that the observed time constant of the water level increase is explained by the time constant of the well-aquifer system. The water pressure increase caused by the seismic waves is probably attributed by weakening of the solid phase of aquifer, like a liquefaction process.

Reference

Takahide Yokoyama, Shigeo Odaka, Kazuhiro Itadera, Kazuo Nagase and Shigeo Sugiyama, Monitoring system and analysis of groundwater level for investigating the method to predict Western-Kanagawa Earthquake, Report of Hot Spring Research Institute of Kanagawa Prefecture, Vol.26, No.1, pages 21-36, 1995

K. Karasaki, J. C. S. Long, and P. A. Witherspoon, Analytical Models of Slug Tests, Water Resources Research, Vol.24, No.1, pages 115-126,1988

Changes in groundwater chemistry at the Taiwan Chelungpu Fault Borehole before the 2013 M6.2 Nantou earthquake

Ching-Chou Fu[1], Chun-Wei Lai[2], Tsanyao Frank Yang[2], Cheng-Hong Chen[2], Kuo-Fong Ma[3], Lou-Chuang Lee[1]

1. Institute of Earth Sciences, Academia Sinica, Taiwan
2. Department of Geosciences, National Taiwan University, Taiwan
3. Department of Earth Sciences & Institute of Geophysics, National Central University, Taiwan

Key words: Chelungpu Fault Drilling Project (TCDP), Nantou Earthquake, Precursor

Monitoring of groundwater chemistry in seismically-active regions has been carried out since the 1980s in Taiwan. Change in groundwater chemistry has been observed before earthquakes and is proposed as a precursor signal. However, the biweekly/monthly sampling interval were commonly performed, some short-term precursory anomalies may not be caught due to the low sampling frequency. We designed an automatic sampling apparatus for the retrieval and temporal analysis of water geochemistry. The device was composed of the syringes connected to glass bottles with the septum for collecting fluids each day, which was installed at the Chelungpu Fault Drilling Project (TCDP) drilling well in central Taiwan for observing the discharge of fluids. The stable isotope ratios for oxygen and hydrogen anomalies of ~ +0.6‰ and +2.0‰, respectively, relative to the local background measured in groundwater were observed as the potential seismic precursor, one month before the Nantou earthquake (M6.2) in central Taiwan. The findings could be explained by the mixture between the different chemical concentrations from groundwater and surrounding formation through water-rock interaction, which may be associated with pre-seismically induced changes of permeability or opening of preexisting micro-fractures along the fault zones due to high fluid pressure. We suggest that geochemical anomaly in groundwater could be useful for future researching on the earthquake precursor.

The preliminary study of the coseismic groundwater level changes in M_L 6.2 Hualien earthquake, Feb. 6 2018

Wen-Chi LAI[#+], Shih-Jung WANG[*], Kuo-Chin HSU, Chjeng-Lun SHIEH

National Cheng Kung University, Taiwan

[*]*National Central University, Taiwan*

[#]*Corresponding author: laiwenji@dprc.ncku.edu.tw* [+]*Presenter*

The different response by various natural stimuli and processes (tidal force, barometric loading, ground shaking and crustal strain) were used as the elements of the hydraulic information in the earthquake induced groundwater level changes. Using the natural force to act as naturally recurring stimuli to provide a sufficiently varied distribution of excitations in time and space, and represented the hydro-geological changes responses to the earthquake processes. The purposes of this study are to analyze the recently observation results of the earthquake induced pre-seismic / co-seismic variation of groundwater level M_L 6.2 Tainan earthquake, Feb. 6 2018. The analysis of the high-sampling water level responses be used to estimate the mechanical properties of the aquifer. Comparison the observation high-sampling water level changes in the each event, offers the opportunity to discussion the possible mechanism of the hydrologic response to earthquake. Some of the coseismic groundwater level changes can be explained as the poroelastic responses to the earthquake-induced volumetric strain changes inferred from the fault dislocation models. But the other changes can not be explained by the volumetric strain changes either qualitatively or quantitatively. We regarded the coseismic static volumetric strain change and the ground acceleration as the main factors to cause the coseismic groundwater level changes. The study provides some information for the pre-seismic / co-seismic mechanism but more investigations are required.

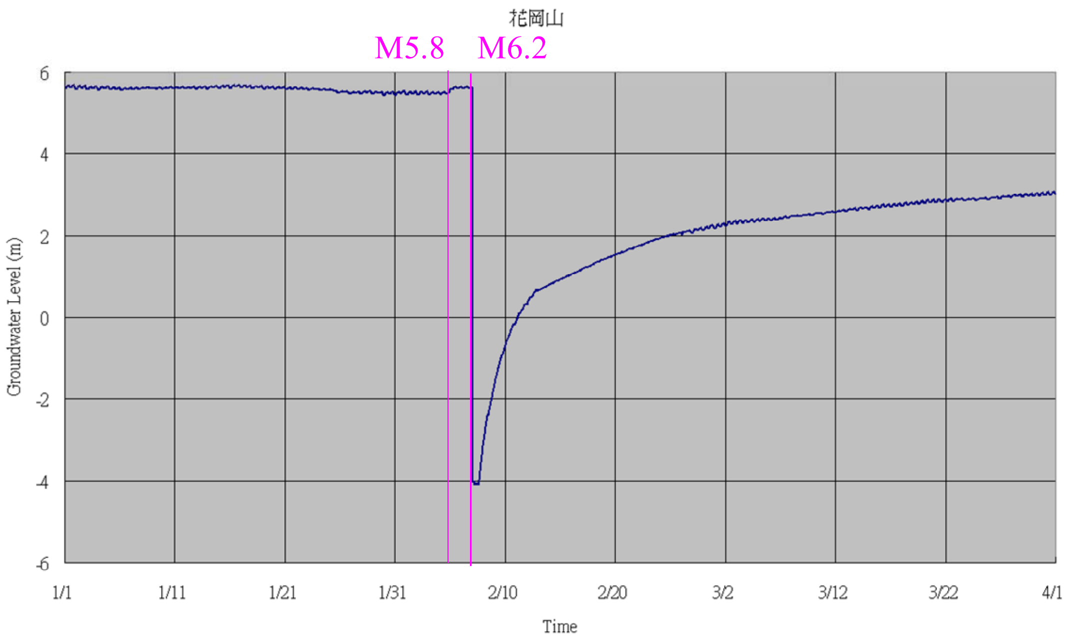

Figure 1. The coseismic groundwater level changes in M_L 6.2 Hualien earthquake, Feb. 6th 2018

Postseismic changes in stream water related to the 2016 Kumamoto earthquake

*N. Koizumi[1], T. Ajiki[1], A. Mori[1], T. Sato[2], H. A Takahashi[2], N. Matsumoto[2],and K. Kawabata[3]

1. School of Environmental Science, the University of Shiga Prefecture,
2. AIST, Geological Survey of Japan, Research Institute Earthquake and Volcano Geology,
3. Graduate School of Science and Engineering, Kagoshima University

1.Introduction

It has been well known that large earthquakes sometimes cause hydrological changes widely in and around the region of strong ground motion. In many cases of those changes, stream flow and spring flow increases in lowland and water table drops in highland. Those changes sometimes continued for a period of several months to years (Rojstaczer and Wolf ,1992; Sato et al., 2000) . Since Japan is relatively rich in water resources, people may have not paid much attention to these earthquake-related hydrological changes in Japan. But those hydrological changes are clearly one of the seismic risks and should also be examined in Japan.

There were two main events of the 2016 Kumamoto earthquake, ie, the foreshock of M (magnitude) 6.5 on April 14, 2016 and the main shock of M 7.3 on April 16, 2016. The 2016 Kumamoto earthquake produced the surface earthquake fault and the wide region of the seismic intensity upper 6. Both of them reached Mt.Aso. The 2016 Kumamoto earthquake also caused many changes in stream water and groundwater (Sato et al., 2017; Ichiyanagi and Ando, 2017). In our presentation we will mainly report the postseismic changes in stream water related to the 2016 Kumamoto earthquake.

2.Method

There are two main rivers in and around Kumamoto city. One is the Shirakawa river system and the other the Midorikawa river system. We mainly analyzed the data of stream flow in those rivers which are open on the internet (MLIT, 2018). We also analyzed the data of the 11 spring waters where we surveyed 7-12 times during the period from 2014 to 2017.

3.Result and Discussion

After the 2016 Kumamoto earthquake, the flow rate increased for a few month in the rivers whose upper basin is Mt.Aso.

Three main hypotheses for the earthquake-related hydrological changes have been suggested, ie, (1) Static coseismic elastic strain changes caused by earthquake-related crustal deformation (Muir-Wood and King, 1993), (2) Liquefaction caused by strong ground motion (Manga, 2001), and (3) Permeability enhancement caused by strong ground motion (Rojstaczer et al, 1995). Recently vertical permeability enhancement of the mountain in upper river basin has been strongly suggested (Wang et al., 2010; Wang and Manga, 2015).

The hypothesis (1) seems to be denied because distribution of the coseismic volumetric strain changes caused by the foreshock and the main shock did not correspond to the stream flow changes. The distribution did not also correspond to the flow rate changes of spring waters (Sato et al., 2017). The hypothesis (2) also seems to be denied because the flow rate in some rivers from the liquefaction area of the 2016 Kumamoto earthquake (Wakamatsu et al., 2017) did not change. In addition, it seems difficult for liquefaction to cause stream flow increases for a few month because liquefaction generally ends soon after earthquake ground motion. The hypothesis (3) can explain this case. As described above, the surface earthquake fault and the region of the seismic intensity upper 6 reached Mt. Aso. Therefore it is considered that permeability enhancement at Mt. Aso can explain the post seismic change in the stream water.